

Article

Development of a Thermal Environment Analysis Method for a Dwelling Containing a Colonnade Space through Coupled Energy Simulation and Computational Fluid Dynamics

Tatsuhiko Yamamoto ^{1,*}, Akihito Ozaki ² and Myonghyang Lee ³

¹ Architecture and Equipment Engineering, Kurume Institute of Technology, Kurume 8300052, Japan

² Graduate School of Human-Environment Studies, Kyushu University, Fukuoka 8190395, Japan

³ Department of Science and Engineering, Ritsumeikan University, Kusatsu 5258577, Japan

* Correspondence: ymt@kurume-it.ac.jp; Tel.: +81-0942-22-2345

Received: 14 May 2019; Accepted: 1 July 2019; Published: 3 July 2019



Abstract: In building design, several approaches have been proposed for coupling computational fluid dynamics (CFD) and energy simulation (ES) to perform analyses of thermal environments. The unsteady analysis of thermal environments within buildings containing offices and colonnade spaces is difficult to perform using an ES that represents the space with a single mass point, owing to excessive predictive heat loss; therefore, CFD has typically been used instead. Although it is possible to divide the space into zones using ES, it leads to excessive predicted heat loss and the prediction of heat movement due to the influence of strong air currents, such as those associated with air conditioners. This behavior is observed because these zones are not detailed mesh divisions. To solve these problems, we proposed a method for calculating the ratio of heat contribution to zones that were pre-divided using CFD followed by the distribution of the total thermal load calculated by ES. In this study, we proposed a method for coupling ES and CFD, which enabled the unsteady analysis of a thermal environment in a large space and verified its accuracy.

Keywords: ES; CFD; large space; heat loss

1. Introduction

The behaviors of thermal environments are typically predicted using computational fluid dynamics (CFD), a specialized approach to solving flows of physical quantities based on energy simulation (ES) and incorporating fluid dynamics based on heat transfer theory. This approach has been developed and used for a significant length of time in the building industry. Detailed instantaneous thermal environment predictions are possible using CFD. However, when performing long-term unsteady analysis, the calculation load is decreased by using ES to perform calculations for the thermal performance of spaces using a single mass point system. Typically, ES and CFD are useful when applied in appropriate situations.

As a traditional ES calculation method, radiation calculations can be examined in detail using the form factor. In recent years, it has also become possible to consider the effects of sunshine and shadows, thereby improving the calculation accuracy.

However, general ES input conditions include not only weather conditions, but convective heat transfer rate and transfer flow rate. When a space is divided into zones, these values are unknown and conventional values are used.

On the other hand, in the conventional CFD calculation method, the calculation load is extremely high when the number of meshes is high. This is because repetitive calculations will need to be performed using the SIMPLE method, which is not suitable for long-term non-stationary calculations.

Moreover, the coupled simulation of convection and radiation is possible, however, the calculation load is further increased because the radiation calculation routine is included in the convergence calculation of the convection.

CFD is a useful tool because it allows an understanding of the thermal distribution of a space by reducing the calculation load, but it is difficult to use it in isolation because it is necessary to calculate boundary conditions separately. This is the current state of the industry.

Many research projects have been conducted related to energy conservation using ES alone. In addition, research into coupling with equipment models is also currently in progress. In terms of CFD-only research, the method of establishing boundary conditions is very haphazard, and there are multiple items that cannot be adjusted without prior experience, such as turbulence models applied when analyzing spaces such as atriums. Because the application of CFD requires boundary conditions to be established, it is desirable to calculate these conditions using ES and then to couple these two approaches by passing these data over to the CFD model. The application range for ES and CFD coupling includes attempts to calculate and couple CFD boundary conditions using ES, not only in indoor environments, but also on an urban scale [1]. An ES and CFD coupling method for use in indoor environments was presented by Zhai et al. The surface temperature was calculated using CFD, the convective heat transfer coefficient was then calculated and the two were coupled together and convergence was established. This method was termed sequential time static coupling [2,3]. This approach is coupled with an advancing time step without the need to perform dynamic calculations and convergence calculations. Because dynamic coupling typically requires the performance of convergence calculations at every given time step, the CFD computational load can be problematic in terms of the attendant computational cost [4,5]. In a few decades, the constraints associated with technological development related to design work will involve satisfying certain requirements, such as increasing energy conservation standards. In these circumstances, static coupling could help to minimize computational loads and may this recommend its use as a desirable option.

As an aside, the definition of the convective heat transfer coefficient differs depending on the commercially available software package; hence, it is difficult to apply this practically in terms of versatility.

In addition, Zhai et al. [6] presented a detailed definition of the convective heat transfer coefficient in terms of the coupling of ES and CFD [6] in a scalable commercially available software package (e.g., Star-CD [7], Fluent [8], or OpenFOAM [9]). It is, however, difficult to apply this without CFD that is applied using a suitable source code such as [10,11]. Therefore, in this study, we have developed technology based on static coupling.

In static coupling, an attempt is made to calculate the thermal stratification to be analyzed by applying boundary conditions calculated using ES to the CFD model. However, CFD is not suitable for unsteady analysis due to its high computational load, making it difficult to evaluate the period of thermal stratification. To analyze large spaces such as open spaces and offices, ES usually assumes 10 or 20 air-changes per room volume, because the transfer rate between arbitrarily divided zones is unknown [12]. It is difficult to predict actual physical phenomena using assumed values. To solve this problem, a method of dividing the space into layers and calculating the heat transfer between zones as a block model [13,14] has been developed, but there are many associated input conditions that require adjustment, and considerable experience is thus required. Therefore, it is not particularly practical.

In recent years, coupled analysis has been conducted to calculate the flow rate between zones using CFD and then to transfer it to ES [15]. Nonetheless, this coupled method still makes assumptions regarding the precision of data for office spaces, including such assumptions as the fact that the air-conditioning is supplied by a plurality of air conditioners, or that the environment possesses excellent natural convection. However, in an environment where the air flow is dominant, such as in

air-conditioned spaces, the ES side zone division tends to overestimate the amount of advection heat with directivity, and the temperature immediately below the outlet may become too high. To address this issue, we calculated the rate at which heat input from the air conditioner reached each zone using CFD and developed a method for distributing the total heat load calculated using ES. In a similar study, Sasayama et al. calculated the thermal response in a fixed flow field using CFD and developed a calculation method for thermal stratification to be incorporated into ES [16]. However, the incoming heat flow included convective and radiative heat. It was separated into transmissions, potentially leading to the generation of differing results using this calculation method for convective heat transfer.

In addition, the contribution ratio of indoor climate (CRI) [17–19], which represents the sum of individual heat sources contributing to the formation of a temperature distribution developed by Kato et al., is a method of analyzing an arbitrary point in space, so a zone such as defined in an ES model is targeted. In this case, it is necessary to integrate the calculated values for the measurement points of the zone. The method used in this study specialized in calculating the temperature of the zone with a small attendant calculation load. The total heat load, calculated by ES in this study, was distributed using the heat contribution rate for each zone, calculated using CFD. It was then injected into each zone as the amount of input heat for the ES to solve the heat balance for the space on a continuous moment-by-moment basis. A simple calculation method was developed to calculate the temperature.

2. Theoretical Background to the Proposed Method

2.1. Difference in Simulation Calculations Using Various Heat Flow Paths

A comparison of heat flow paths was performed using ES as shown in Figure 1. It was possible to capture detailed arbitrary physical quantities in three dimensions through mesh division of the space using CFD. ES was not suitable for predicting three-dimensional distribution characteristics because it expresses space with one mass point.

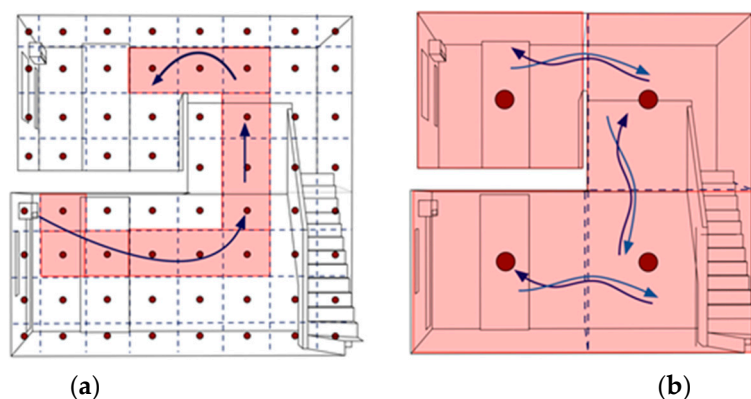


Figure 1. The diffusion of heat using CFD and ES. (a) Heat flow path using CFD; (b) Heat flow path using ES.

In this study, we analyzed a residential building containing a colonnade space. The proposed method divided the large space into regions using ES and then used CFD to calculate the advection between the zones and expressed the diffusion of heat from heat sources using ES once again. However, as with floor heating, because heat was propagated by natural convection, it was possible to analyze this with high accuracy if it was not gently spread out with mass. It was difficult to ascertain the precision of the calculation without detailed mesh divisions in an environment where advection, such as that associated with an air conditioner, was dominant. ES is based on the supposition of instantaneous heat diffusion, so in the case of heat diffusion over greater distances via advection, additional heat is input into the space directly under the air inlet which does not reach distant areas.

We calculated the contribution of heat to each zone as divided by the ES, using CFD to avoid such a problem in this study. We developed a coupled method that enabled the unsteady analysis of the period of each zone using ES. Hereafter in this document, the terms 1F and 2F refer to the first and second floors of the building model used in this study, respectively.

In this study, it was assumed that warm air moved from 1F to 2F during heating, through diffusion of heat from the outlet due to the influence of the air conditioner air flow. Therefore, there was a possibility that the amount of heat in the zone right under the outlet would be over-estimated in the amount of coupled advection between zones. We confirmed that it was valid for the verification of the proposed method and we selected it as a target.

2.2. Proposed Method

The basic concept behind the coupling method proposed in this study is shown in Figure 2. The proposed method clarifies the thermal contribution of each arbitrarily divided zone through separate CFD analysis of the thermal diffusion by advection due to the air conditioner. This solves the problem associated with ES mentioned in the previous section. By dividing the amount of heat in each zone by the amount of heat input by the air conditioner, the amount of heat input to the zone could be represented by a ratio.

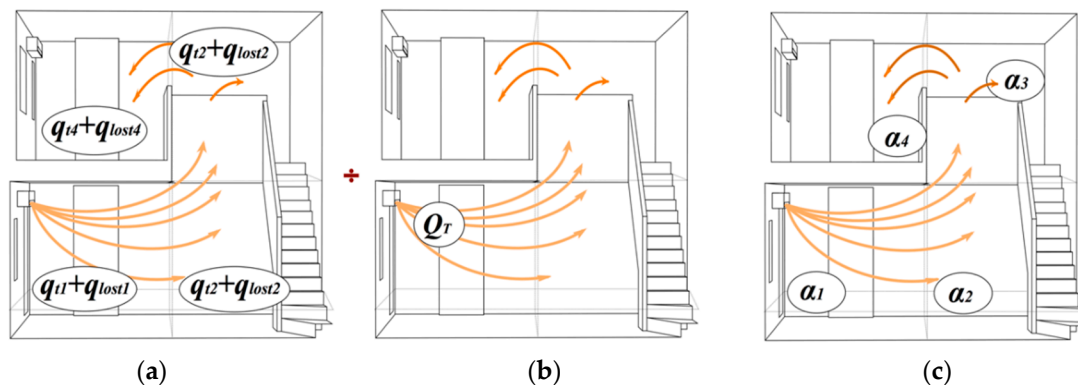


Figure 2. Conceptual diagram of the proposed method. (a) Calculation of heat quantity using CFD; (b) The heat input by the air conditioner; (c) Coefficient of thermal diffusion.

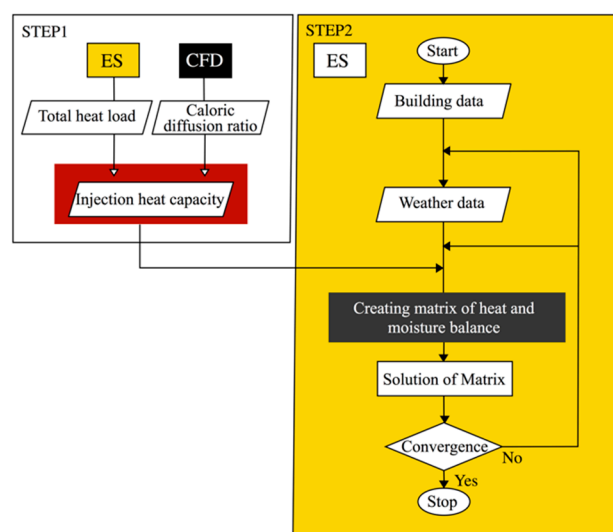


Figure 3. Computational flow chart for the proposed method.

Figure 3 shows a flow analysis for the proposed method. In STEP 1, ES is used to calculate the total thermal load at each moment. The coefficient of thermal diffusion, indicating the quantity of heat

reaching each zone, was calculated using CFD. By multiplying the total thermal load by the coefficient of thermal diffusion, the heat input to each zone was calculated using ES. In STEP 2, the caloric value is calculated as the amount of heat input into the ES from moment to moment within each zone.

2.3. Proposed Calculation Method

The coefficient of thermal diffusion is the ratio of the thermal contribution to each zone. The coefficient of thermal diffusion for each zone is expressed by Equation (1):

$$\alpha_i = \frac{C_p \gamma V_i \frac{(T_i - T_{s,i})}{dt} + q_{losti}}{Q_T} \quad (1)$$

The reference state was taken as the thermal environment when the amount of input heat was set to 0. The heat associated with the rise in temperature, obtained by differentiating the deviation from the thermal environment at the time of actual heat input with respect to time, was added to the heat loss from the zone's wall surfaces and was assigned as the net heat input to each zone. The thermal diffusion contribution from each calculated air inlet to each zone was divided by the total amount of heat input by the air inlet, and was defined as the coefficient of thermal diffusion.

As expressed in Equation (2), when the coefficients of thermal diffusion of each zone are added together, the total is unity:

$$\sum_{i=1}^n \bar{\alpha}_i = 1 \quad (2)$$

The amount of heat input to each zone using ES is shown in Equation (3):

$$q_i = L \cdot \alpha_i \quad (3)$$

The momentary total heat load previously calculated using ES was multiplied by the coefficient of thermal diffusion and distributed to each zone. The final heat balance of the space, taking into account the amount of heat distributed to each zone, is shown in Equation (4). The amount of heat input to the space was the sum of the heat transfer by convection from the wall surfaces, the heat exchange with the outside air, and the heat input to each zone calculated using Equation (3):

$$V_{ol} c \gamma \frac{dT_i}{dt} = \sum_{j=1}^J S_{i,j} h_{i,j} (T_{i,j} - T_i) + V_{oc} \gamma (T_o - T_i) + q_i \quad (4)$$

The amount of heat input to the space was the sum of the heat transfer by convection from the wall surfaces, the heat exchange with the outside air, and the heat input to each zone calculated using Equation (3).

3. Simulation Measurement and Analysis Conditions

3.1. Outline of Target Laboratory Housing and Measurement Points

Figure 4a,b show the 1st and 2nd floor plan (1F and 2F) and actual measurement points of the experimental housing. Although the experimental housing was three stories in height, partitions were set up in the staircase between the 2nd and 3rd floors, and only the 1st and 2nd floors were measured. In addition, the 2nd floor living room also contained partitions in the same position as the staircase. There was a staircase with a stairway on the 1st floor which was adjacent to the living room on the 2nd floor. In addition to the convection type air conditioner (room air conditioner) and the radiant heating panel, under-floor heating was laid in only one room on each floor with an attendant floor laying rate of 70%. These rooms are marked by the shaded areas in Figure 4. At each measurement point,

the in-space temperature, the surface temperature, the air movement speed, and the globe temperature were measured at one-minute intervals.

The measurement points a1 to d were four points at heights of floor level (FL) + 100 mm, +600 mm, +1100 mm, +1700 mm. The measurement points LD 1 and LD 2 were at heights of FL + 0 mm, +100 mm, +600 mm, +1100 mm, +1700 mm, +2300 mm, +2400 mm. The measurement point LDwh included 9 points at heights of FL + 0 mm, +100 mm, +600 mm, +1100 mm, +1700 mm, +2800 mm, +3800 mm, +5000 mm, and ceiling level (CL)-0. The measurement points f to i were at heights of +5 points of 100 mm, +650 mm, +1200 mm, +1750 mm, and CL - 100 mm, and were used to measure the vertical temperature distribution of the space. The average outer heat transmission coefficient of the actual experimental house used in this experiment was $U - A = 0.58 \text{ W/m}^2 \cdot \text{K}$. The average outer heat transmission coefficient was $U - A = 0.6$ in accordance with the ZEH standard for areas 4 to 7 in the energy conservation standard area classification. The building was a high insulation house that satisfied the requirements for $\text{W/m}^2 \cdot \text{K}$.

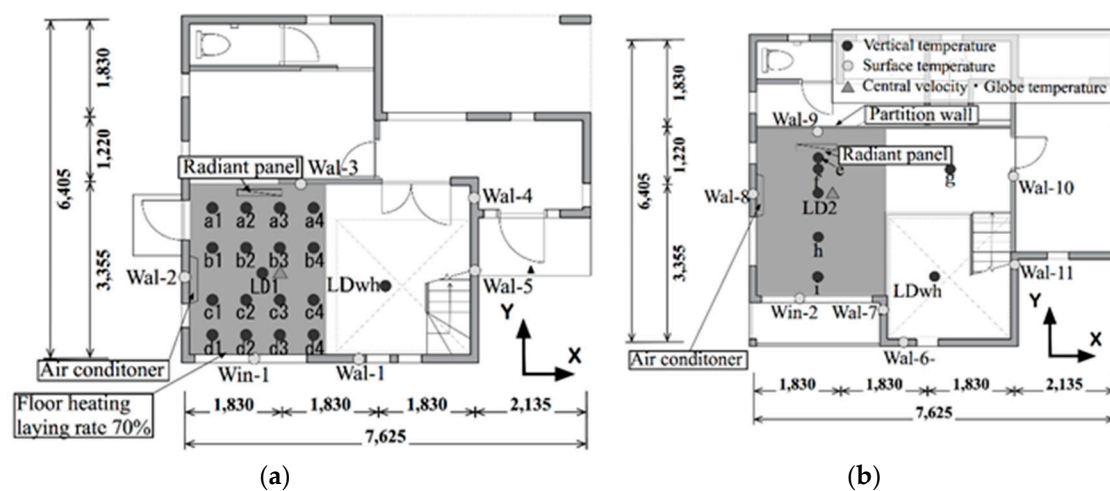


Figure 4. Heat diffusion using CFD and ES. (a) Experimental house 1st floor (1F); (b) Experimental house 2nd floor (2F).

3.2. Outline of Actual Measurement Process

The experimental conditions are shown in Table 1. For the weather conditions in the winter experiment, both the temperature and the relative humidity were set to the average value for the month of January in Fuchu-shi, Tokyo. The air conditioner was set to 20 °C and the air flow direction was set to 30° downward from the air conditioner outlet. The air movement speed (air volume) of the air conditioner was set to “strong”.

Table 1. Experimental conditions.

| Artificial Weather Room Setting | Tokyo Prefecture Fuchu City |
|---------------------------------|--|
| Ventilation frequency | 0 times |
| Air conditioner model number | 1F:S50FTSP-W (Opening area:0.049 m ²) 2F:S28FTSS-W (Opening area:0.063 m ²) |
| Setting | Winter |
| Temperature | 20 °C |
| Air inlet angle | 30° from the horizontal plane |
| Air inlet speed | Strong |

The experimental case conditions are presented in Table 2. In the winter conditions, we conducted two case experiments: Case 1, which included the operation of convection type air conditioners on both the 1st and 2nd floor, and Case 2, where a convection type air conditioner was only operated on the 1st floor. When it was detected that the room temperature sensor built into the indoor unit reached the set temperature, the convection type air conditioner sent a control signal to stop the operation of the compressor of the outdoor unit for energy conservation purposes. In this experiment, the radiant heating panels and underfloor heating were not in operation, only the convection type air conditioners were in continuous operation. Only the outside air temperature and humidity were controlled as variables in the artificial weather room, sunlight and wind speed were not taken into consideration. In this experiment, the outdoor temperature was caused to fluctuate periodically and steadily, and analysis was carried out with the results being utilized after 1–2 days, after the behavior of the air conditioner was seen to be sufficiently stable. In this experiment, Case 1 was conducted over a total of 5–6 days, with a 1-day run-in period, a 2-day run-up period, and a 4-days measurement period.

Table 2. Experimental Case.

| Weather Conditions | Case | Convection Air Conditioner Operation Status | |
|--------------------|-------|---|----|
| | | 1F | 2F |
| Winter | Case1 | ○ | ○ |
| | Case2 | ○ | |

3.3. Analysis Model and Calculation Conditions

In this study, we used the dynamic thermal load calculation software package, THERB for HAM [20], for the prediction and analysis of the temperature, the humidity of the entire building considering heat, moisture, and air coupling. CFD modelling was performed using the commercial software package STAR-CCM + [21]. The analysis model constructed in THERB is shown in Figure 5a. The space from the base to the second floor was divided into partitions that could be analyzed, and the numbers in the figure indicate the numbering chosen for each zone. General zone division in ES was performed for each room in use, or was flexibly changed based on the item under consideration. Therefore, the first floor was divided vertically into two layers at a height of FL + 450 mm for the purposes of checking the influence of the cold draft near the floor. The analysis model used in CFD is shown in Figure 5b. In THERB, the modeling was done with a certain degree of simplification due to the characteristics of ES, but in the STAR-CCM program, CFD modeling was done in detail as one of the aims was grasping the distribution characteristics due to diffusion from the air inlet.

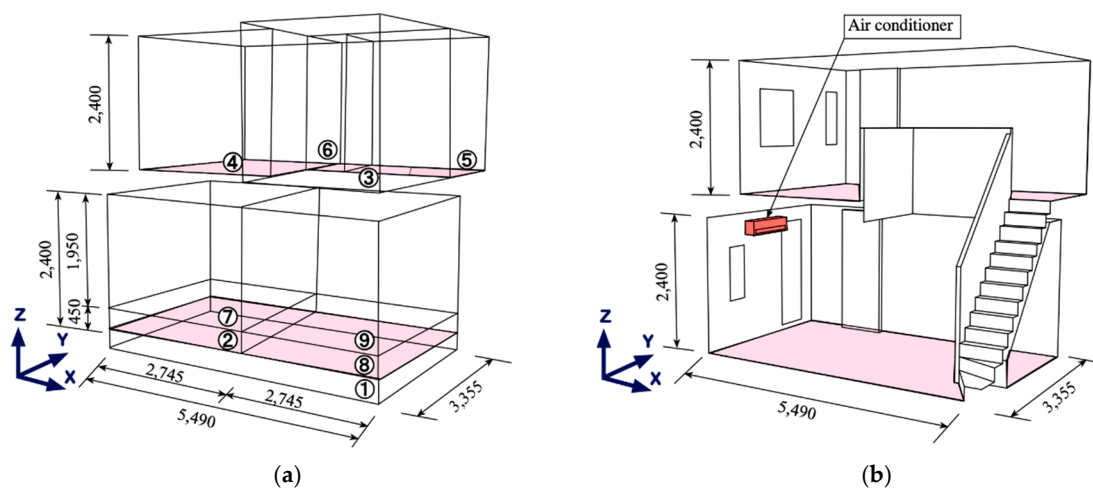


Figure 5. Analysis model for ES and CFD. (a) Zoning of ES; (b) CFD analysis model.

We also modelled stairs and waist walls to analyze the effect of downward flow. Table 3 shows the calculation conditions for THERB. One of the calculation conditions was that the air conditioner on only one floor was in operation in both summer and winter. The weather data for THERB and the amount of heat input from the air conditioner in STEP 1 were measured values. With respect to the CFD boundary conditions in terms of air inlet, the air flow velocity was calculated using the air inlet and air outlet temperature as known conditions from the total thermal load calculated using THERB.

Table 3. ES analysis condition.

| Item | Conditions |
|------------------------------------|---|
| Calculation time interval | 10 minutes interval |
| Weather data | Measured value (temperature and humidity) |
| Ventilation frequency | 0.2 air changes/h |
| Room occupants | None |
| Air conditioning set temperature | Measured value |
| Heat input during air conditioning | See Figure 8 |

Table 4 shows the analysis conditions for CFD. Because the analysis method proposed in this study had to incorporate the calculation of heat loss from the walls, we divided the first layer of the wall finely. Although consideration of the computational load is necessary when considering practical applications of the proposed method, this study focused on verification of the accuracy of the proposed method. Detailed temperature stratification was thus calculated without using the wall function.

Table 4. CFD analysis conditions.

| Item | Conditions |
|-----------------------|---|
| Turbulence model | Low Re type k- ϵ model |
| Mesh number | Approximately 3.2 million mesh elements |
| Air inlet angle | 30° |
| Air inlet temperature | 318.15 K |
| Air inlet velocity | 2.4 m/s |
| Calculation code | STAR-CCM+11.02.010 |

4. Verification of the Accuracy of the Proposed Method

4.1. Procedure for Verifying Accuracy of the Proposed Method

The calculation procedure was roughly divided into three parts: Verification of the accuracy of the simulation, verification of the accuracy of the proposed method, and application examination of the proposed method. In the simulation accuracy verification, we reported the estimation of the unknowns using THERB and the verification of the accuracy of the CFD using the estimated physical values and the measured values as boundary conditions. In the accuracy verification of the proposed method, we presented the calculation of the distribution coefficient and the verification of its accuracy. In the application study of the proposed method presented in the next section, we reported the sensitivity analysis using the air inlet angle and the confirmation of the reproducibility of the temperature stratification of the colonnade space at the time of operation of both air conditioners.

4.2. Estimation of Unknowns Using THERB

Figure 6 shows the area-weighted average value of the inner surface temperatures of the THERB calculated value and the measured value. The measured values and the surface temperature from

THERB were roughly similar; however, slight differences were seen in Room 2 and Room 8. It was proposed that this was because the temperature under the floor was not included as an input condition, which differed from the actual measurement situation.

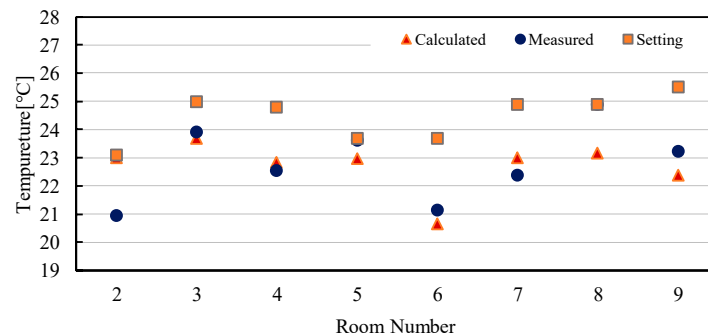


Figure 6. Verification of accuracy of air conditioning set temperature and surface temperature.

The variation in the thermal load over time is shown in Figure 7. This thermal load was multiplied by the coefficient of thermal diffusion and distributed to each zone.

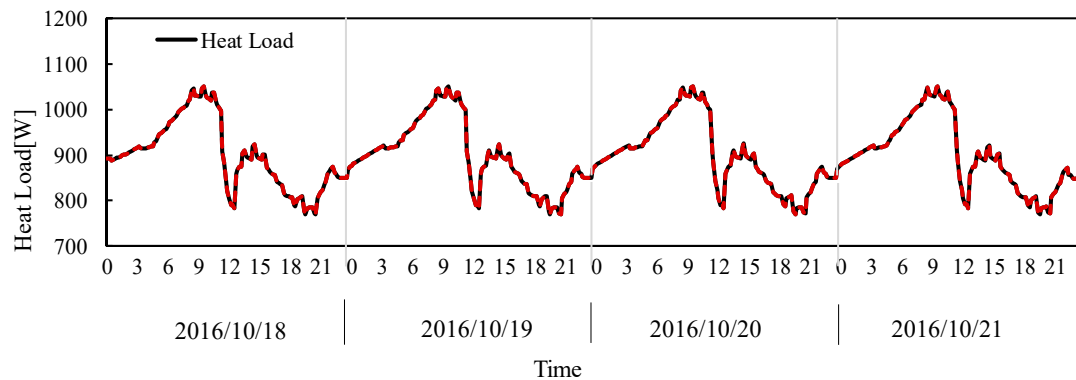


Figure 7. Result for the calculation of the amount of input heat.

The momentary flow velocity was calculated using Equation (5) with the measured value of the air inlet temperature and the air outlet temperature as known conditions. Because the time variation was not large, an average value of 2.4 m/s was adopted:

$$v = \frac{q_T}{C_{air} \gamma A_{air} (T_{air} - T_{su})} \quad (5)$$

4.3. Confirmation of CFD Accuracy Using Measured Values

The accuracy of the contribution of the air inlet to each zone as calculated using CFD requires that the initial temperature distribution of the space be correct. Therefore, accuracy verification was carried out using the flow velocity as calculated in Section 4.2 and the surface temperature based on the measured values as boundary conditions.

Figure 8 shows the accuracy verification results of the temperature distribution characteristics of each zone of the CFD. The values calculated using CFD agreed with the measured values with a high degree of accuracy. Although a deviation of approximately 0.8 °C was noted in the temperature of Room 8, it was confirmed that this was within the allowable range because the errors associated with the measuring equipment were large at the volume-weighted average temperature. That is, an error occurs because the volume of the divided area of the area is represented by one measurement point (the error of the measurement device alone is ±0.5 °C). In addition, since the true value is not known, it is difficult to completely trust the volume-weighted average temperature because the error may

propagate. Figure 9 shows the comparison between the measured and calculated air outlet temperature at an air inlet angle of 30°. The error between the actual measurement value (25.7 °C) of the air outlet temperature and the calculated value (26.0 °C) confirmed the high accuracy of the measured value, which possessed a margin of error of 0.3 °C. It was also confirmed that the flow rate calculated using THERB and the total thermal load were correct.

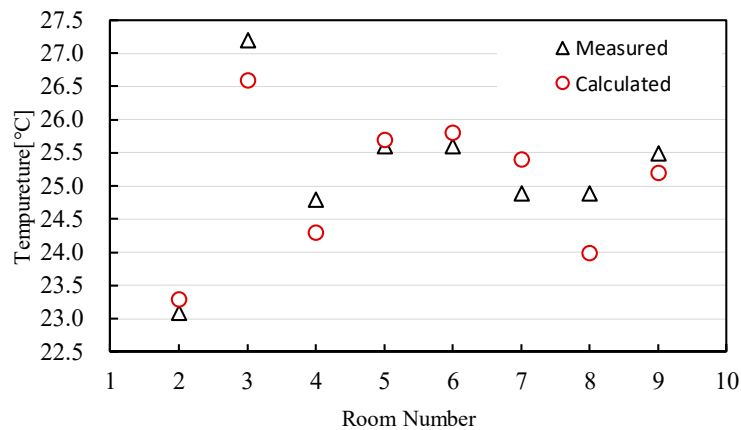


Figure 8. Correspondence between the values calculated using CFD and the measured values in each zone.

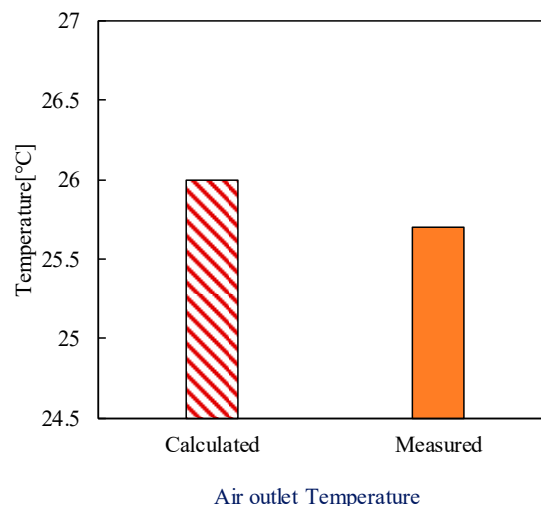


Figure 9. Comparison of calculated and measured air outlet temperatures at an air inlet angle of 30°.

4.4. Calculation of Distribution Coefficient

We used the surface temperature calculated in Section 4.2 to calculate the distribution coefficient, taking into consideration the cases where the heat load was at either a maximum or minimum. The boundary conditions of CFD at the lowest load are shown in Figure 10. The high correlation between the measured and calculated values confirmed that the boundary conditions were appropriate. The coefficient of thermal diffusion at the lowest load is shown in Figure 11. The coefficient of Room 3, which is a high air-flow space, is the highest, and it could be confirmed that the heat moved by convection. As for Room 5 and Room 6, the heat spread to influence the zone of the next room through the air inlet and thus demonstrated higher values. It was confirmed that the difference between the maximum and minimum load was not too large. The CFD analysis result is shown in Figure 12. It could be confirmed that heat was transported to Room 4 of 2F due to the air flow from the air conditioner of Room 7 of 1F.

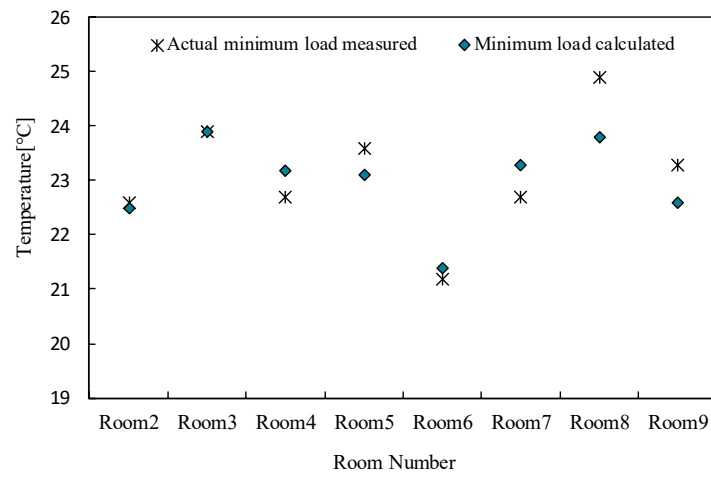


Figure 10. CFD surface temperature boundary condition.

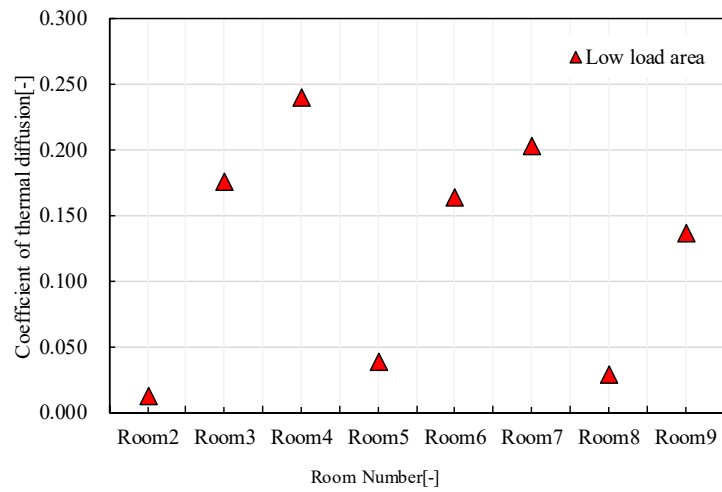


Figure 11. Coefficient of thermal diffusion of each zone.

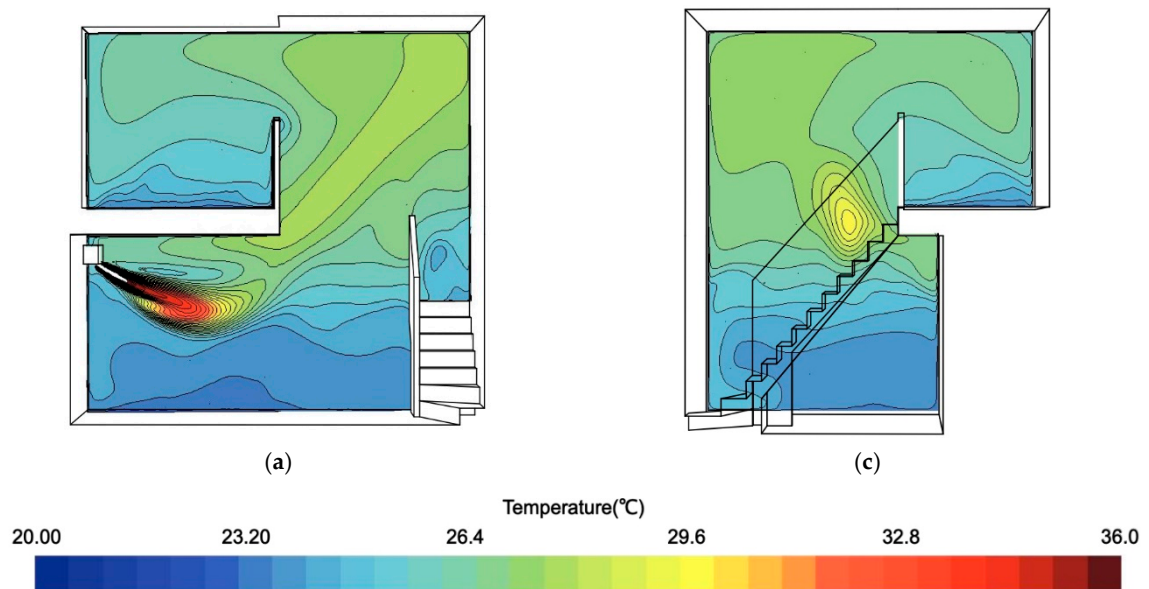


Figure 12. Cont.

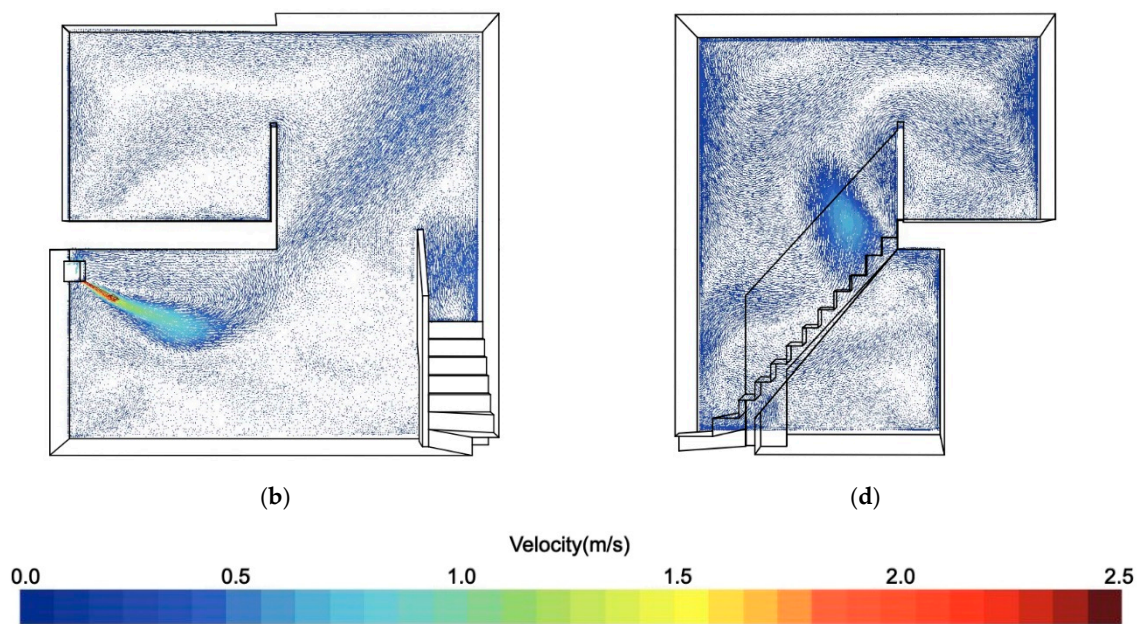


Figure 12. CFD analysis results. (a) Y = 1.5 m Temperature distribution; (b) Y = 1.5 m Air speed distribution; (c) Y = 3.27 m Temperature distribution; (d) Y = 3.27 m Air speed distribution.

4.5. Accuracy Verification of Distribution Coefficient

Figure 13 shows the room temperature of each zone of the THERB model along with the room temperature at the time of measurement. The input heat was the amount of input heat divided by the coefficient of thermal diffusion, taking into consideration the influence of the air conditioner air flow using CFD.

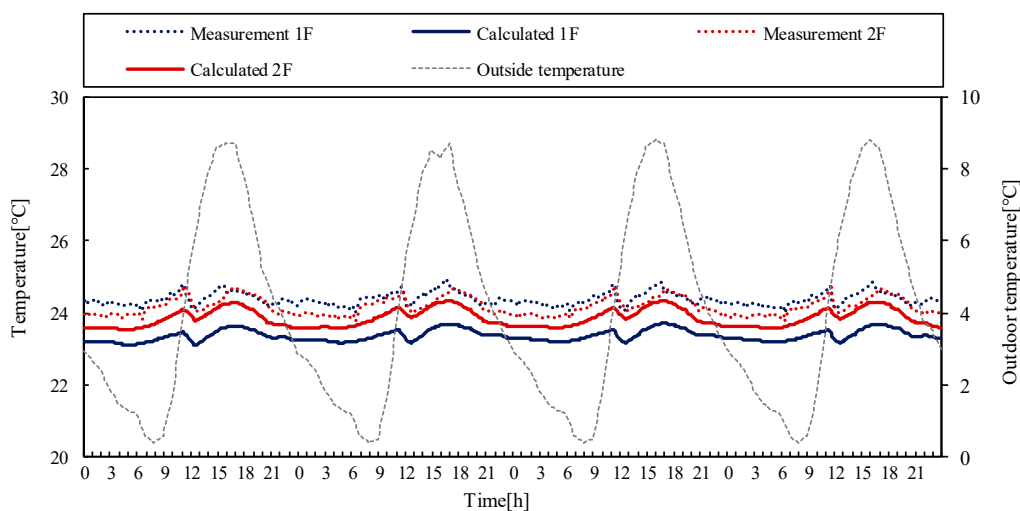


Figure 13. Accuracy verification result.

Although there was an error of approximately 1 °C in the maximum load time zone in Room 7, Room 4 fell within an error margin of approximately 0.6 °C. In the lowest load time zone, an error of approximately 0.7 °C occurred in Room 7 and an error of approximately 0.5 °C occurred in Room 4. A further difference between 1F and 2F can be seen in Figure 14. The actual heat load measurement value of each zone was set as the heating set temperature of the THERB at the minimum load time. This was the heat quantity actually required. The amount of input heat consisted of the product of specific heat, specific gravity, and the flow rate with the total load and CFD air inlet and outlet temperature difference. These were integrated values for each zone calculated by THERB in comparison

with the reference heat quantity. The amount of input heat was distributed using the coefficient of thermal diffusion. Comparing the results, it was confirmed that both THERB and CFD generated the reference heat accurately. This result supported the validity of the coefficient of thermal diffusion.

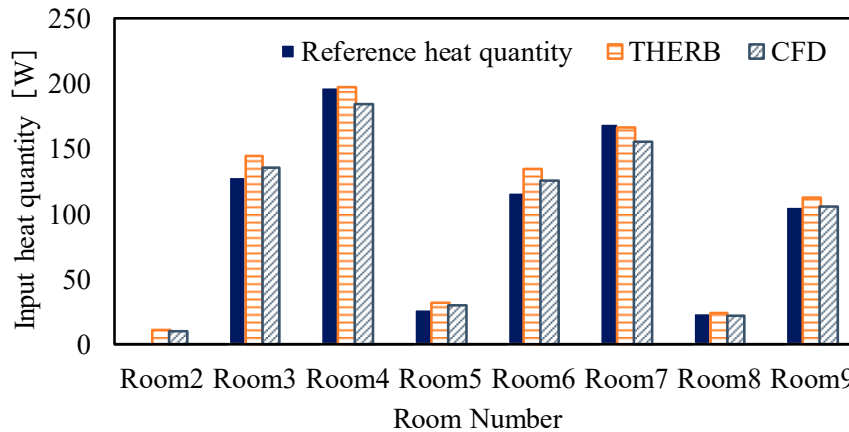


Figure 14. Accuracy verification of heat transfer coefficient.

4.6. Sensitivity Analysis by Air Inlet Angle

When the proposed method was used, it was possible to predict that the indoor thermal environment fluctuated due to variables such as the air inlet angle, the swing angle, and the air volume. With regard to the air inlet velocity, additional analysis was required because the influence of the air conditioner was reduced when the energy conservation mode was set. However, because ES and CFD need to be linked sequentially, the focus in this study was on verification of the accuracy of the proposed method. The abovementioned additional study items were thus excluded from this study. In this study, sensitivity analysis was performed using the air inlet angles that were considered to be most commonly used. To simplify the comparison, the analysis was performed at $\pm 10^\circ$ with the median angle chosen as the accuracy verification case. The difference between the specific temperature and the specific weight multiplied by the difference between the air inlet temperature and the air outlet temperature caused the air outlet temperature to change as the air inlet angle changed, so the heat input varied with the air inlet angle.

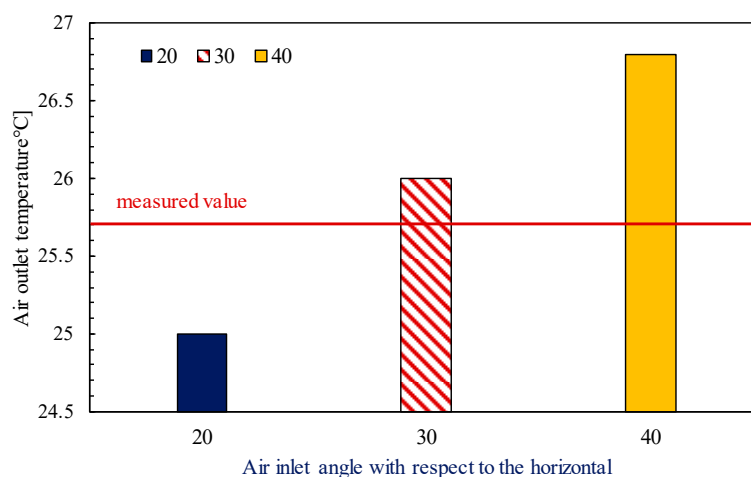


Figure 15. Comparison of air outlet temperature by sensitivity analysis.

If the amount of heat input varies, it means that two variables would be used as part of the analysis conditions, compromising the planned sensitivity analysis. The air inlet temperature was changed by combining the amount of input heat with a 30° air inlet angle, which could not be compared without

matching the amount of input heat. The convergence calculation was performed using CFD until the amount of input heat fell within an error margin of 8%. A comparison of the air inlet angle and the air outlet temperature is shown in Figure 15.

In the cases of the calculated values for air inlet angles of 20° and 40°, comparison with the measured values showed that the air outlet temperature was lesser or greater than the measured value, and the error was ± 0.7 °C. The result confirmed that an air inlet angle of 30° yielded the most similar calculated value in comparison with the measured value. The reason that the air outlet temperature tended to be high when the air inlet angle in the horizontal direction was large was proposed to be due to the influence of convection. The coefficients of thermal diffusion for various air inlet angles are shown in Figure 16.

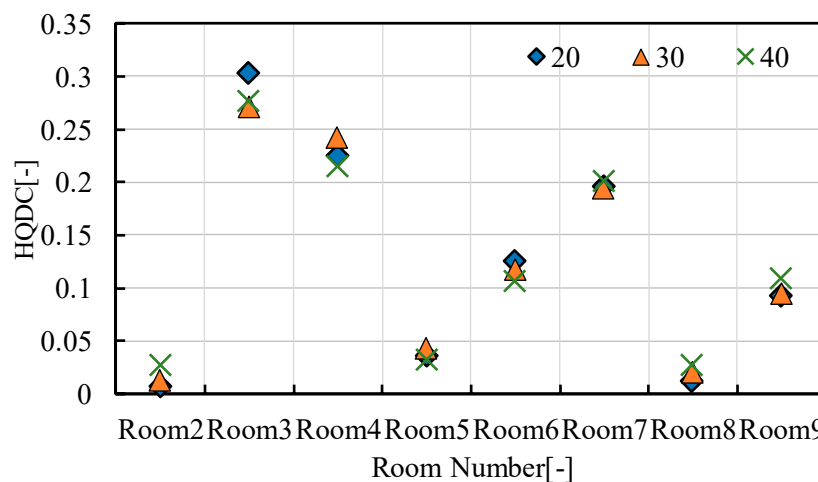


Figure 16. Comparison of coefficient of thermal diffusion using sensitivity analysis.

It was confirmed that the same tendency was observed at 20° and 40° as compared with the standard 30° case. It was proposed that it would change depending on the amount of heat input, rather than on the air inlet angle, and it could be predicted that it would depend largely on the flow rate. The sensitivity analysis results are shown in Figure 17. The temperature of the main room tended to be higher in the case where the air inlet angle was 20°. This was considered to be so because heat was distributed to a zone such as Room 2 when the air inlet angle became large. In fact, such a tendency can be seen in Figure 18. However, the temperature scale was within a range of approximately 0.5 °C, and even when the air flow direction changed, no significant differences were observed.

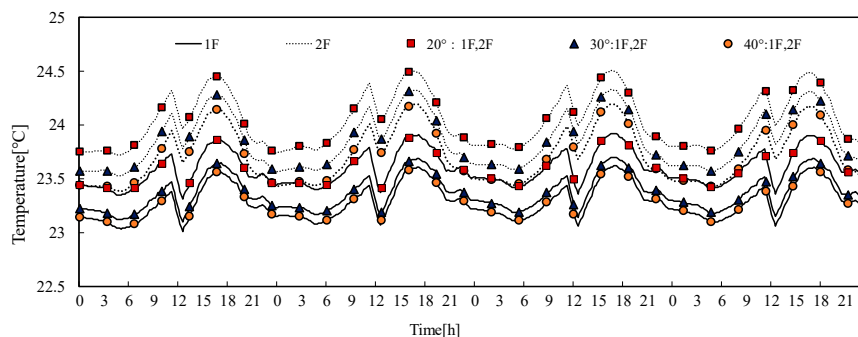


Figure 17. Sensitivity analysis results for air flow direction.

4.7. Confirmation of Heat Source Addition

The validity of the proposed method was confirmed with one air conditioner operating in Sections 4.1–4.5. Understanding the contribution to the space from heat sources when two air

conditioners were operating in the open space was also useful for design and other practical purposes. Thus, in this section, the thermal contribution to each zone with two operating air conditioners was confirmed with accuracy verification, using the actual values and the proposed method.

In the calculation using ES, it was difficult to determine which air conditioner had processed the calculated heat load. Even if the heat diffusion by the air conditioner advection transported the heat to 2F while 1F was air conditioned, it was difficult to distribute the heat when the 2F air conditioner was also operating. Therefore, in this study, the correct distribution heat quantity was calculated using the heat source addition depicted in Figure 18.

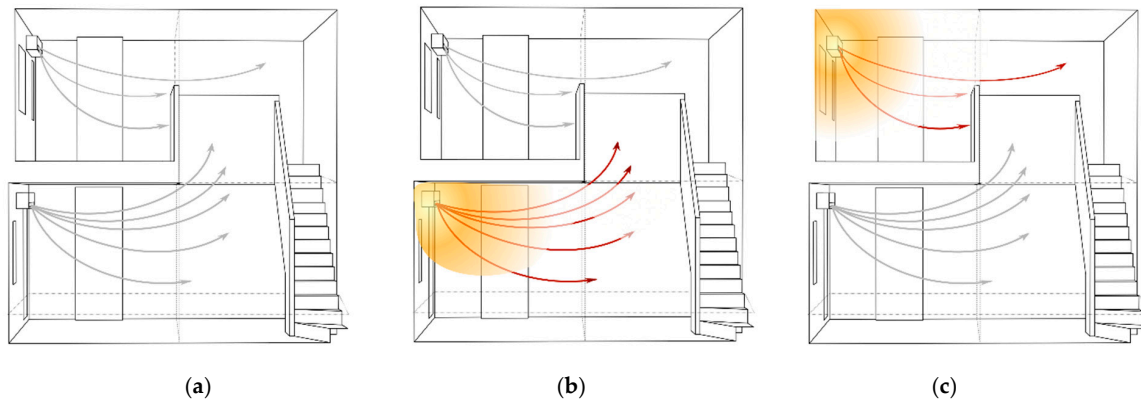


Figure 18. Depiction of heat source addition. (a) Reference condition (heat input 0 W); (b) Only 1F heat input; (c) Only 2F heat input.

Initially, the amount of heat present when the floors were divided into 1F and 2F using zone division, was input into the air conditioner to perform CFD analysis. By providing the flow rate to the air conditioner which had not injected the amount of advection heat, the amount of heat input for each floor and its thermal contribution to each zone was confirmed and the net amount of heat was evaluated by performing the following steps:

- (1) The heat transfer coefficient was calculated for each floor.
- (2) The amount of input heat of the temporary air conditioner was distributed using the coefficient of thermal diffusion
- (3) The heat input was added to each zone calculated for each floor and added as the net heat input
- (4) The convergence calculation was performed for heat input
- (5) Accuracy verification was conducted for the main rooms

The convergence calculation is expressed by Equation (6):

$$Q_r = q_r + q_h \quad (6)$$

It is clear from the CFD analysis results shown in Figure 19 that the heat from the air conditioner of 1F was also carried to 2F. Therefore, the amount of heat contribution to 2F was calculated using the coefficient of thermal diffusion calculated from results of the analysis performed after assigning the amount of heat to the 1F air conditioner. The total amount of heat was obtained by adding them. In addition, the amount of heat that contributed to 1F at the time of operation of the 2F air conditioner was similarly added. The heat quantity of the 2F air conditioner was calculated using the same procedure. The calculated heat quantity was distributed using the coefficient of thermal diffusion to obtain the amount of ES input heat.

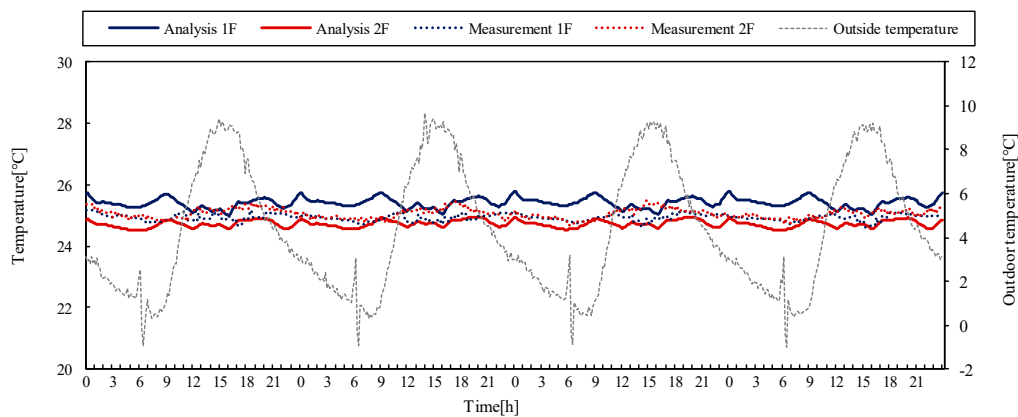


Figure 20. Accuracy verification result of heat source addition.

The temperature difference noted in the distribution between 1F and 2F when two air conditioners were in operation was small. It can be seen from Figure 19 that the air inlet flow velocity was different. This was due to the fact that the heat loads for 1F (480.7 W) and 2F (560.6 W) were different and that the opening area of the air conditioner outlets were different. From the calculation results, the flow rate for 1F was 1.29 m/s, and for 2F was 1.6 m/s. The flow rate for the air conditioner on each floor was calculated using Equation (5) presented in Section 4.2. It was determined that the heat loads and heat transfer coefficients of 1F and 2F were correct because they were confirmed by the fact that the actual value was duplicated by the accuracy verification result for the heat source addition as shown in Figure 20. The calculated value for the coefficient of thermal diffusion for each floor is shown in Figure 21. The heat transfer by the air conditioner affected Room 4 when the air conditioner operated on 1F. It could also be confirmed that it affected 1F when the air conditioner operated on 2F because of the heat transfer coefficient of Room 4 (2F) and Room 7 (1F), which were the main rooms. It was proposed that this was because heat was transported to an area other than the air conditioned floor by the advection of the air conditioner. It was difficult to calculate heat load using ES when forced convection prevailed and heat transfer was performed in a continuous manner in zones such as high air-flow spaces.

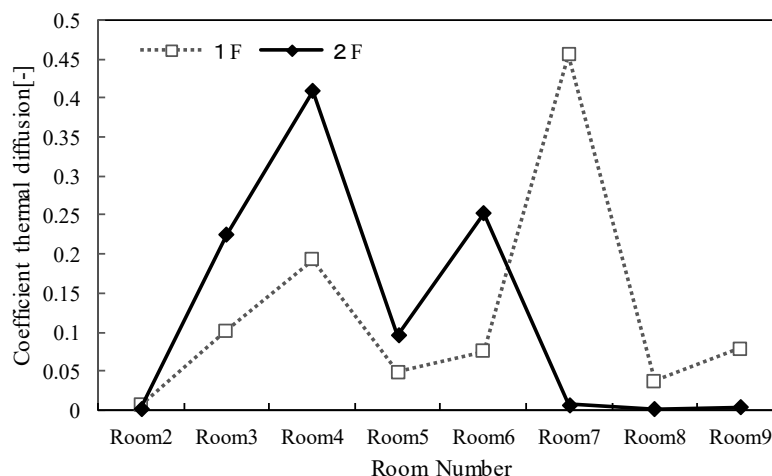


Figure 21. Coefficient of thermal diffusion of each floor.

5. Conclusions

In this study, the heat transfer from heat sources was calculated using CFD and ES with the contribution to each zone divided arbitrarily, overcoming the difficulty associated with the prediction of indoor thermal environments with excellent forced convection. We proposed a ratio-based method

for distributing the heat load calculated using ES. To confirm the accuracy of the coefficient of thermal diffusion used in the proposed method, after confirming the accuracy of the software package, THERB, the calculation was performed as a boundary condition of CFD, and the accuracy of CFD was confirmed. In addition, sensitivity analysis using air flow direction was conducted to investigate the influence of air flow direction on each zone. Furthermore, to confirm whether the addition of heat sources was effective, the coefficient of thermal diffusion was calculated for each floor. The heat load was then distributed and the accuracy of the room temperature in the main living room was confirmed. The following findings were obtained from the above study:

- (1) The boundary conditions (surface temperature and air conditioner flow velocity) for CFD were calculated using THERB, and it was confirmed that the calculated surface temperature was almost identical to the measured value. Additionally, we calculated the momentary amount of heat input and confirmed that the air conditioning set temperature was reached with only a small amount of heat input (approximately 1300 W) because the insulation performance was very good.
- (2) The coefficient of thermal diffusion was calculated using CFD from physical quantities such as heat loss through the walls and the temperature of each zone. It was confirmed that the temperature of the main living room could be accurately predicted. The heat input was compared with the accuracy of the coefficient of thermal diffusion.
- (3) Sensitivity analysis was conducted to investigate the influence of the air inlet angle on the room temperature. When the air inlet angle was 30°, little difference existed between the actual measured value of the air outlet temperature and the measured value, and it was also confirmed that the amount of input heat was appropriate to apply as a measurement condition. It was confirmed that the air outlet temperature tended to increase as the air inlet angle in the horizontal direction increased. It was confirmed that the coefficient of thermal diffusion demonstrated little fluctuation due to the air inlet angle and was within the range of approximately ± 0.5 °C as a temperature range.
- (4) The convergence calculation was performed by calculating the coefficient of thermal diffusion when the heat quantity calculated using THERB was input to the air conditioner of each floor to confirm that the heat sources could be added. The method of distributing the heat load was verified. By performing a convergence calculation for the purpose of calculating the heat load of each floor using ES, it was found that the room temperature of the main living room demonstrated an average error of approximately 0.3 °C.

Author Contributions: Conceptualization, T.Y. and A.O.; methodology, T.Y.; software, T.Y.; validation, T.Y.; formal analysis, T.Y.; investigation, T.Y.; resources, M.L.; data curation, T.Y.; writing—original draft preparation, T.Y.; writing—review and editing, M.L.; visualization, T.Y.; supervision, A.O.; project administration, M.L.; funding acquisition, A.O. and M.L.

Funding: This research received no external funding.

Conflicts of Interest: The authors declare no conflict of interest.

Nomenclature

| | |
|-------------|---|
| α | Coefficient of thermal diffusion [–] |
| C_p | Specific heat of air [J/kg·K] |
| γ | specific gravity [kg/m ³] |
| V_i | iZone volume [m ³] |
| T_i | iZone temperature [K] |
| $T_{s,i}$ | iZone reference temperature [K] |
| q_{losti} | Heat loss from the wall [W] |
| Q_T | Amount of input heat of air conditioner [W] |
| C_{air} | Specific heat of air conditioner inlet air [J/kg·K] |
| A_{air} | Air outlet area [m ²] |

| | |
|---|---|
| T_{air} | Air outlet temperature [K] |
| T_{su} | Air outlet port air temperature [K] |
| $T_{i,j}$ | Room i, temperature of target element j [K] |
| \bar{c}_γ | Apparent volumetric specific heat of rooms containing furniture [J/m ³ ·K] |
| $S_{i,j}$ | Area of room i, target element j [m ²] |
| $h_{i,j}$ | Convective heat transfer coefficient of room i, target element j [W/m ² ·K] |
| V_o | Ventilation rate with the outside air [m ³ /s] |
| C_γ | Volumetric specific heat of air [J/m ³ ·K] |
| q_i | i Zone heat load [W] |
| v | Air inlet speed [m/s] |
| L | Total heat load [W] |
| T_{air} | Outlet temperature [K] |
| T_s | Air outlet temperature [K] |
| q_r | Heat quantity of r floor [W] |
| Q_r | Sum of heat load of each zone at the time of air-conditioner operation of the r floor distributed by coefficient of thermal diffusion [W] |
| q_h | Sum of the heat quantity of each zone transported to the h floor when the r floor air conditioner was distributed according to the coefficient of thermal diffusion [W] |
| Contribution ratio of indoor climate (CRI) | When multiple heat sources are present, a standard flow field is created and fixed to calculate the thermal contribution to the space per heat source. CRI is a method for predicting the temperature at any point by adding the temperatures at any point together |
| Coefficient of thermal diffusion (α) | In energy simulation (ES), thermal diffusion is difficult to calculate, and the effect of strong directional advection is calculated beforehand by computational fluid dynamics (CFD) and is reflected in the non-stationary calculation of ES. The influence of the air conditioning advection on the zone that divides the space arbitrarily can be considered, which is convenient for the ES. |

References

- Jonas, J.C. Simulations of local heat islands in Zurich with coupled CFD and building energy models. *Urban Clim.* **2018**, *24*, 340–359.
- Zhai, Z.; Chen, Q.; Haves, P.; Klems, J.H. On approaches to couple energy simulation and computational fluid dynamics programs. *Build. Environ.* **2002**, *37*, 857–864. [[CrossRef](#)]
- Zhai, Z.; Chen, Q. Solution characters of coupling between energy simulation and CFD programs. *Energy Build.* **2003**, *35*, 493–505. [[CrossRef](#)]
- Zhai, Z.; Chen, Q. Performance of coupled building energy and CFD simulations. *Energy Build.* **2005**, *37*, 333–344. [[CrossRef](#)]
- Zhai, Z.; Chen, Q. Sensitivity analysis and application guides for integrated building energy and CFD simulation. *Energy Build.* **2006**, *38*, 1060–1068. [[CrossRef](#)]
- Zhai, Z.; Chen, Q. Numerical determination and treatment of convective heat transfer coefficient in the coupled building energy and CFD simulation. *Build. Environ.* **2004**, *39*, 1001–1009. [[CrossRef](#)]
- STAR-CD. Available online: https://mdx.plm.automation.siemens.com/ja_jp/star-cd (accessed on 9 May 2019).
- ANSYS-Fluent. Available online: <https://www.ansys.com/ja-jp/products/fluids/ansys-fluent> (accessed on 9 May 2019).
- Openfoam. Available online: <https://openfoam.org> (accessed on 9 May 2019).
- Mathieu, B.; Sigrid, R. Coupling building energy simulation and computational fluid dynamics: Application to a two-storey house in a temperate climate. *Build. Environ.* **2014**, *75*, 30–39.
- Pan, Y.; Li, Y.; Huang, Z.; Wu, G. Study on simulation methods of atrium building cooling load in hot and humid regions. *Energy Build.* **2010**, *10*, 1654–1660. [[CrossRef](#)]
- AE-Sim/HeatCatalog. Available online: <http://www.ae-sol.co.jp/aesol02.html> (accessed on 9 May 2019).
- Togari, S.; Arai, Y.; Miura, K. Simplified Prediction Model of Vertical Temperature Distribution in a Large Space: Study on a thermal environment design system for large spaces, Part 1. *J. Archit. Plan. Environ. Eng. AIJ* **1991**, *427*, 9–19.

14. Togari, S.; Arai, Y.; Takemasa, Y. Application of Mathematical Model for Unsteady State Heat Analysis of Large Space to Existing Atrium, Including Prediction of Vertical Air Temperature Distribution: Study on a thermal environment design system for large spaces, Part 3. *J. Archit. Plan. Environ. Eng. AIJ* **1994**, *455*, 23–30. [[CrossRef](#)]
15. Yamamoto, T.; Ozaki, A.; Lee, M.; Kusumoto, H. Fundamental Study of Coupling Methods between Energy Simulation and CFD. *Energy Build.* **2018**, *159*, 587–599. [[CrossRef](#)]
16. Hiyama, K.; Kato, S. Integration of three-dimensional CFD results into energy simulation utilizing an advection-diffusion response factor. *Energy Build.* **2011**, *43*, 2752–2759. [[CrossRef](#)]
17. Kato, S.; Murakami, S.; Kobayashi, H. New Scales Assessing Contribution of Heat Sources and Sinks to Temperature Distributions in Room by Means of Numerical Simulation. In Proceedings of the Fourth International Conference on Air Distribution in Rooms (ROOMVENT'94), Rakow, Poland, 15–17 June 1994; pp. 1–19.
18. Zhang, W.; Hiyama, K.; Kato, S.; Ishida, Y. Building energy simulation considering spatial temperature distribution for nonuniform indoor environment. *Build. Environ.* **2013**, *63*, 89–96. [[CrossRef](#)]
19. Matsumoto, T.; Kato, S.; Sasamoto, T.; Omori, T. Proposal of Coupling CFD with Energy Simulation by CRI, Fundamental research on the coupled simulation of CFD and energy simulation (Part 1). *J. Archit. Plan. Environ. Eng. AIJ* **2008**, *73*, 445–450.
20. Ozaki, A. Prediction of Hygrothermal Environment of Buildings Based Upon Combined Simulation of Heat and Moisture Transfer and Airflow. In Proceedings of the International Building Performance Simulation Association, Montréal, QC, Canada, 15–18 August 2005; pp. 899–906. Available online: http://www.ibpsa.org/proceedings/BS2005/BS05_0899_906.pdf (accessed on 3 July 2019).
21. STAR-CCM. Available online: https://mdx.plm.automation.siemens.com/ja_jp/star-ccm-plus (accessed on 9 May 2019).



© 2019 by the authors. Licensee MDPI, Basel, Switzerland. This article is an open access article distributed under the terms and conditions of the Creative Commons Attribution (CC BY) license (<http://creativecommons.org/licenses/by/4.0/>).